

# MAGNETIC DRUM STORAGE APPLIED TO SURVEILLANCE RADAR

R. M. Page

Associate Director of Research  
for Electronics

and

S. F. George

Consultant, Radar Division

January 31, 1957



APPROVED FOR PUBLIC  
RELEASE - DISTRIBUTION  
UNLIMITED

NAVAL RESEARCH LABORATORY  
Washington, D.C.

## CONTENTS

Abstract	ii
Problem Status	ii
Authorization	ii
<b>INTRODUCTION</b>	<b>1</b>
<b>DESCRIPTION OF STORAGE DRUM SYSTEM</b>	<b>1</b>
The Input	2
The Storage	2
The Output	5
<b>RANGE AND RANGE RESOLUTION</b>	<b>6</b>
<b>RANGE RATE AND DOPPLER RESOLUTION</b>	<b>7</b>
<b>STORAGE REQUIREMENTS</b>	<b>10</b>
<b>BANDWIDTH REQUIREMENTS</b>	<b>10</b>
<b>DYNAMIC RANGE REQUIREMENT</b>	<b>11</b>
<b>A NUMERICAL EXAMPLE</b>	<b>13</b>
<b>AZIMUTH DETERMINATION</b>	<b>15</b>
<b>CONCLUDING REMARKS</b>	<b>15</b>
<b>ACKNOWLEDGMENTS</b>	<b>16</b>
<b>APPENDIX A - Obtaining The Doppler Frequency</b>	<b>17</b>
<b>APPENDIX B - Resolution Criterion</b>	<b>19</b>
<b>APPENDIX C - Power Spectra</b>	<b>22</b>
<b>LIST OF SYMBOLS</b>	<b>23</b>

## ABSTRACT

A long-range surveillance radar has been proposed in which a high-speed, rotating magnetic drum is used for information storage. The magnetic drum techniques make possible high range-rate resolution at all ranges and high output signal-to-noise ratio without the need for banks of narrow output doppler filters. The radar is basically of the pulse-doppler type wherein range resolution is a function of the transmitted pulse duration and range-rate resolution is determined by the integration time; i.e., the length of time the input information is stored on the magnetic drum.

In order to exploit the storage capacity to the ultimate, very short samples of the received pulses are recorded on the drum in a stepped-sequential manner in order to cover all of the range gates. At the same time, the totality of stored pulses is read off successively, once for each doppler gate, and mixed with a swept local oscillator to provide range-rate resolution in a continuously running system. The operation of the storage system is analyzed in detail. In addition to determining the limits of range and range-rate resolution of which the system is capable, the bandwidth and dynamic range requirements are established.

## PROBLEM STATUS

This is one of a series of reports on this problem; work is continuing.

## AUTHORIZATION

NRL Problem R02-23  
Project NR 412 000  
Subproject NR 412 007

Manuscript submitted December 20, 1956

## MAGNETIC DRUM STORAGE APPLIED TO SURVEILLANCE RADAR

### INTRODUCTION

The need for surveillance radar capable of target resolution in range rate as well as in range has long been recognized by the Navy. Early efforts to meet the need were devoted largely to moving-target indication, which recognizes only two range rates, one above and one below a range rate arbitrarily selected as the dividing line between moving and stationary targets. This method deteriorates progressively with motion of the radar. Most attempts at greater range-rate resolution have relied on very narrow filters to resolve doppler frequencies in real time and concomitantly to realize all available threshold sensitivity. The number of filters required by such an approach, to span all the doppler frequencies of interest, at all the ranges considered important, and exploiting all the integration permitted by the dynamics of relevant tactical situations, is very large indeed. In order to overcome the difficulties associated with such large numbers of filters, a system was suggested\* in 1954 which makes use of a rotating magnetic drum as a pulse-to-pulse storage medium, from which doppler frequency information is derived sequentially at a substantially accelerated rate. Range-rate resolution and threshold sensitivity are simultaneously maximized by the use of crosscorrelation principles to the limit imposed by tactical situation dynamics.

It must be pointed out that the parameters of currently popular surveillance radar systems do not permit range-rate resolution even remotely approaching the limits imposed by representative tactical situation dynamics, such as the observation time tactically permitted for detection. These limits may be reached when the target is floodlighted; i.e., maintained continuously in the antenna radiation pattern throughout the measurement interval. Conventional scanning techniques therefore are discarded, and the transmitted radiation pattern is fitted to the desired surveillance volume. This may be done without loss of total energy intercepted by a target. Reception may be accomplished with any number of receiver channels, each with its own antenna pattern coverage, the summation of all encompassing the entire surveillance volume. Such a configuration permits maximum range-rate resolution and is assumed in the following description which, for simplicity, is referred to a single receiver channel.

### DESCRIPTION OF STORAGE DRUM SYSTEM

The system is based on the pulse-doppler principle wherein short samples of coherent echo pulses are recorded and stored on a high-speed, rotating magnetic drum. A simplified block diagram of the system is shown in Fig. 1. For convenience of discussion the system diagram has been separated into three parts: the input, comprising the transmitter, antennas, TR, receiver, coherent mixer, and filter; the storage, comprising the sampling circuit and the magnetic drum unit including record and pickoff circuits; and the output, comprising the output local oscillator, doppler filter, detector, and the display unit.

---

\* Proposed by R. M. Page and analyzed by S. F. George.

As discussion of the diagram progresses the method by which the system resolves range and range rate will become evident.

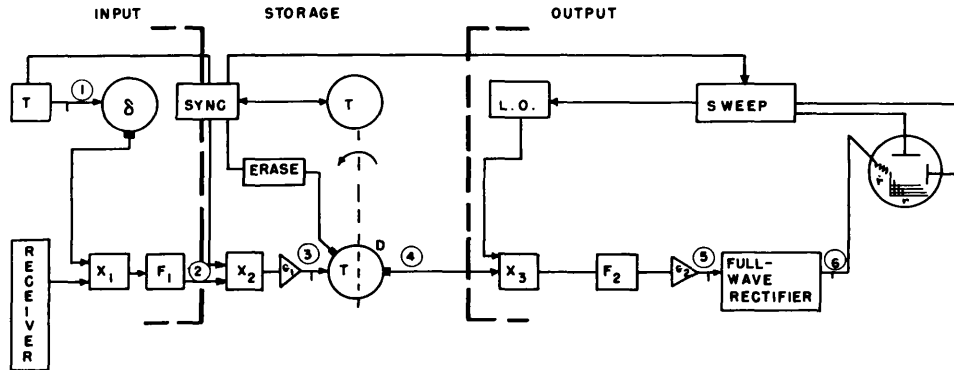


Fig. 1 - Block diagram of magnetic drum storage system

### The Input

The antenna system is not specified precisely beyond prescribing that the transmitted pattern be tailored to the desired surveillance volume and that the received pattern be tailored to the same volume in space or to any desired part of that volume.

The transmitted pulse is stored in a recirculating delay system ( $\delta$  of Fig. 1) where the delay is equal to the pulse length. The stored recirculated pulse, being a replica of the transmitted pulse, provides a noise-free reference for crosscorrelation with received signals. Repetitive "playback" of this pulse into the mixer ( $X_1$ ) and low-pass filter ( $F_1$ ) combination of Fig. 1 gives a complete crosscorrelation between each transmitted pulse and all signals received between that and the succeeding transmitted pulse. Each playback constitutes one range gate. Each new transmitted pulse replaces the last previous pulse in the recirculating delay. The output of filter  $F_1$  is bipolar video which contains doppler frequency information on all targets presented. Doppler frequency appears in the form of modulation of echo height with successive samplings of the same range gate, as described in following sections of this report.

### The Storage

In order to understand the storage part of the system, the short-sample technique will be considered first ( $X_2$  in Fig. 1). Let us consider a simple three-range-gate system and illustrate the bipolar video output resulting first from a stationary target and then from one which has a radial velocity relative to the radar system but which remains essentially in a single range gate during our observation or storage time. A typical noiseless stationary-target case is shown on a continuous time scale in Fig. 2 for an observation time of five received echo pulses. The numbers 1 through 6 at the top of the figure refer to the first, second, etc., transmitted pulses. The lower numbers mark the three range gates. On an A-scope presentation all of the gates marked 1, for example, would fall in the same horizontal location on the cathode-ray tube. The target in Fig. 2 is stationary and is shown to be in the second range gate. A moving target is

illustrated in Fig. 3. Note that the target is located essentially in the second gate during the observation.

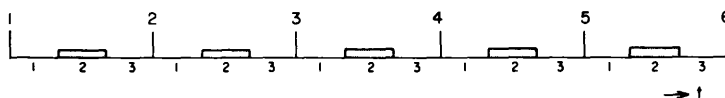


Fig. 2 - Bipolar video from a stationary target

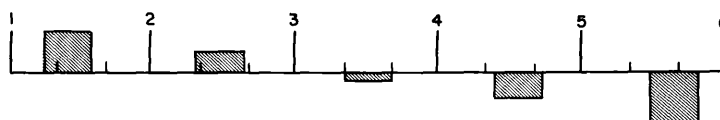


Fig. 3 - Bipolar video from a moving target

There are at least two possible methods of sampling which, on the average, should yield the same results. One is to take each sample from a given range gate at the same point within the gate, say at the center. The second method is to move the sample across the range gate as will be illustrated first for the stationary-target case of Fig. 2. Reference is now made to Fig. 4. A short sample is taken at the beginning of each of the three range gates and the resulting output is labelled 1-1, 2-1, 3-1. Note that for this noiseless case there is zero voltage recorded in the first range gate since there was no echo present at the delay time represented by this gate. On the other hand, there is a voltage recorded in the second range gate indicating the presence of a target. Again there is nothing recorded in the third range gate — meaning no target present. It should be further noted that any voltages present from this first sample must result from a target echo from the first transmitted pulse. The second pulse is now fired and the sampling process is repeated, except that this time the sample is not taken at the beginning of each range gate but instead is shifted over one sample pulse width as illustrated. Once again it is seen that there is a target in the second range gate only. The third pulse is next fired and again the sampling process is repeated moving over another sample pulse width as shown. The whole cycle is repeated for the fourth and fifth transmitted pulses as in Fig. 4.

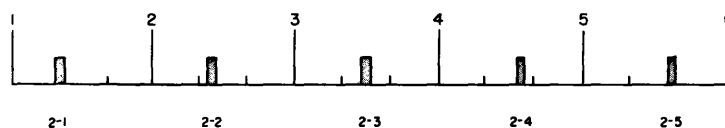


Fig. 4 - Illustration of short-sample technique

Our observation time has now been completely used up; we have sampled the transmitted pulses as many times as is possible, commensurate with the relationship between transmitted and sample pulse widths. How these short samples are processed is illustrated in Fig. 5, which shows the samples as stored on the magnetic drum. In Fig. 1 the sampling rate is shown to be synchronized to the drum rotation and to the pulse repetition frequency. Hence, the first range gate will always be located at the same spot on the drum,

as will the second range gate, etc. In Fig. 5, then, we see how the samples from Fig. 4 are stored sequentially on the drum. The shaded portion in gate 2 signifies that a voltage has been recorded on the drum to indicate the presence of a target.

1					2					3				
1-1	1-2	1-3	1-4	1-5	2-1	2-2	2-3	2-4	2-5	3-1	3-2	3-3	3-4	3-5

Fig. 5 - Illustration of short samples stored on drum

Now a glance at Fig. 5 reveals that the channel has been filled (for this simple five-sample three-gate example). The input pulse samples have been recorded on the drum by gate intervals as follows: 1-1, 2-1, 3-1, 1-2, 2-2, 3-2, ..., 1-5, 2-5, 3-5. When the drum is filled, the pulses are read out successively as follows: 1-1, 1-2, ..., 3-4, 3-5. Thus, in the example of Fig. 5, the three samples 1-1, 2-1, and 3-1 are recorded during one drum rotation, the three samples 1-2, 2-2, and 3-2 are recorded during the second drum rotation, etc.; whereas in read-off all fifteen stored positions are read off during a single drum rotation.

Once the drum is filled, the next step is to erase the oldest information and continue to record the new information. Without regard to the practical difficulty of performing the operation, let us suppose that after the drum has once been filled the oldest samples are erased and the latest recorded. For the moment ignoring any range-gate shift, Fig. 6 shows the result after the sixth drum rotation. We see that the three oldest pulse samples, 1-1, 2-1, and 3-1, have been erased and in their place the three newest pulse samples, 1-6, 2-6, and 3-6, have been recorded. But also note that the range gates are not the same as before, for now gate 1 starts one store position to the right of where it was at first. This means that, in order to locate the range gates correctly, the counting must advance one step on each drum rotation. This is not a problem to the engineer. However, the problem of erasing a single pulse can become a serious one when close spacing is demanded, as normally would be the case here.

1					2					3				
3-6	1-2	1-3	1-4	1-5	1-6	2-2	2-3	2-4	2-5	2-6	3-2	3-3	3-4	3-5

Fig. 6 - Illustration of oldest pulse erasure technique

For illustrative purposes, only three range gates holding only five samples each were considered in Figs. 2 to 6. Now let us generalize to permit surveillance over a total of "g" range gates and let us be capable of storing "I" pulse samples in each range gate.

Then a filled-up channel stretched out in a strip could be represented by the channel strip in Fig. 7. Note that one record head could write-on all the pulses in stepped-sequential fashion and another pickoff head could read off all the pulses successively.

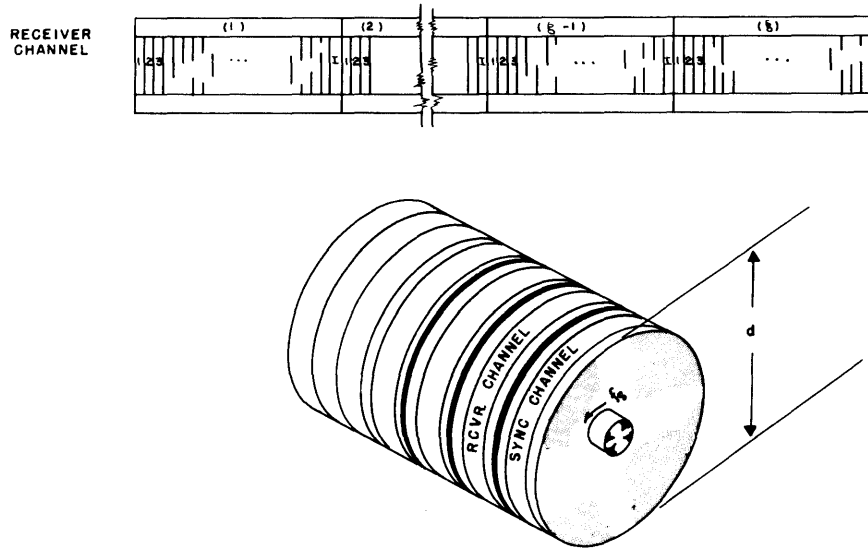


Fig. 7 - Illustration of magnetic drum storage

The tacit assumption has been made in the preceding description that the drum makes a single revolution for each transmitted pulse. Should it not be possible to produce a satisfactory drum rotating at such a high speed, it would be possible to use a slower drum, say  $1/n$ th the "ideal" speed, and record  $n$  sets of range gates on the circumference. Here  $n$  must be an integer. In this case the information from  $n$  pulses instead of that from a single pulse would be recorded for a single complete rotation of the drum.

### The Output

The pulses stored on the drum comprise a carrier signal, on which doppler frequency appears as amplitude modulation. Since all the desired information is contained in the modulation, the output from storage need respond only to the modulation envelope. To determine the frequency of the modulation, the signal from the drum is mixed in  $X_3$  of Fig. 1 with a local oscillator (L.O.) whose frequency is scanned, either continuously or stepwise, through the doppler range. Undesired mixer products are eliminated by a low-pass filter ( $F_2$ ) following the mixer. An output signal from  $F_2$  signifies frequency coincidence between the L.O. and the stored modulation envelope, within the limits of doppler frequency resolution. Doppler resolution is limited ultimately by the duration of the signal in terms of the number of pulses stored in one range-gate interval on the drum. Synchronous inputs to  $X_3$ , displaced 90 degrees, will give no output, resulting in occasional random blind spots. These random blind spots may be eliminated if desired by setting the cutoff frequency of  $F_2$  so that adjacent doppler samplings overlap and each

target appears in two adjacent velocity gates, or by using two mixers in sine-cosine relationship. The output of  $F_2$  is bipolar and may actually alternate during the measurement. However, polarity and frequency have no useful significance at this point, so a full-wave rectifier follows  $F_2$  to simplify presentation problems.

It may now be seen that in one revolution of the drum all range gates are sequentially scanned or "sampled" for one doppler frequency. In succeeding revolutions all range gates "walk" around the drum at the rate of one stored pulse width per revolution, and all are sampled for the next adjacent doppler frequency on each succeeding revolution. In the time interval during which the number of revolutions is equal to the number of samples stored in one range gate, all range gates will have walked one range-gate width around the drum, and all doppler frequencies up to the pulse repetition rate will have been sampled. At this point, the L.O. frequency will return to its starting point and the cycle repeated. This method of operation gives a continuously running system in which all appropriate data are used for each information bit, and no datum is used twice for the same bit, except where velocity gates are made to overlap in order to eliminate the random blind spots.

The display for presenting range and range rate could have a variety of forms. One particularly concise display is indicated in Fig. 1. Here the horizontal sweep is synchronized to the drum rotation, the vertical sweep to the L.O. frequency variation, and the channel output is used to intensity-modulate the screen thus producing range and range-rate information.

## RANGE AND RANGE RESOLUTION

In order to analyze the several important parts of the surveillance system, let us consider the transmission of the pulse sequence shown in Fig. 8 where we define:

$\delta$  = transmitted pulse duration

$\tau$  = pulse repetition period

$f_p$  = pulse repetition frequency =  $1/\tau$ .

It is not the purpose here to consider the factors affecting maximum radar range, as contained in the radar range equation. It will be assumed that the maximum range of the system under discussion is not limited by insufficient power. There is, however, a maximum range dictated by the pulse spacing or pulse repetition frequency. This range arises from the possible ambiguity due to second-time-around echo, a phenomenon familiar to all radar designers. In order to prevent ambiguity, the maximum range,  $r_{\max}$ , is given by

$$r_{\max} = \frac{c\tau}{2} = \frac{c}{2f_p}, \quad (1)$$

where  $c$  is the velocity of propagation. If  $c$  is taken as the velocity of light in free space in nautical miles per second, and if  $f_p$  is in cycles per second then

$$r_{\max} = \frac{8.2 \times 10^4}{f_p}, \quad (2)$$

where  $r_{\max}$  is in nautical miles. This maximum range can be increased in a number of ways, the requirement being twofold: (1) elimination of ambiguity in range by "tagging" the transmitted pulses, (2) maintaining periodicity in transmission so as to preserve doppler information. The difficulty of fulfilling these two requirements in practice may be sufficiently great to suggest using separate systems for added range.

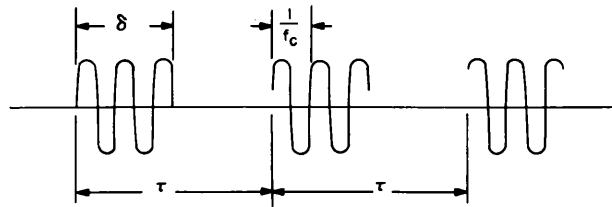


Fig. 8 - Transmitted pulses

Range information is obtained from range gates equivalent in width to the pulse duration. The number of permissible range gates,  $g$ , then, should be the reciprocal of the duty factor, or

$$g \approx \frac{\tau}{\delta} = \frac{1}{\delta f_p} \quad (3)$$

Range resolution is determined by the pulse duration or gate width, and is given by

$$\Delta r = \frac{r_{\max}}{g} = \frac{c\delta}{2} \quad (4)$$

where Eqs. (1) and (3) have been used to obtain the second equality. Again, if  $c$  is the velocity of light in free space and if  $\delta$  is the pulse duration in microseconds, then

$$\Delta r = 0.082\delta, \quad (5)$$

where  $\Delta r$  is in nautical miles. The definition of range resolution used here is in agreement with present-day radar convention.

#### RANGE RATE AND DOPPLER RESOLUTION

A theoretical analysis of how the doppler frequency shift arises for a moving target is presented in Appendix A. For a target moving away from the radar with a radial velocity,  $v_T$ , the shift in frequency due to the doppler effect, which we call the doppler frequency, is given in Eq. (A9) as

$$F = \frac{2f_c v_T}{c}, \quad (6)$$

where  $f_c$  is the transmitted carrier frequency. Since  $v_T$  here represents the time change in radar range, it is actually range rate,  $\dot{r}$ , hence

$$F = \frac{2f_c \dot{r}}{c} \quad (7)$$

If  $\dot{r}$  is in knots and  $f_c$  is in megacycles per second, then

$$F = \frac{\dot{r} f_c}{300}, \quad (8)$$

where  $F$  is in cycles per second. The lower limit to the doppler, for a stationary target, is dc. The highest frequency that need be measured in a pulse-doppler system is dependent upon the pulse repetition frequency. The pulses can be thought of as sampling the doppler and hence, according to Shannon's sampling theorem for distinguishability, there must be at least 2 samples per cycle for the highest frequency; therefore

$$F_{\max} = \frac{f_p}{2} . \quad (9)$$

Input frequencies higher than the critical value will appear in the output as lower frequencies, in the usual manner. Target velocities which produce such frequencies are identified by successive range measurements.

The range rate corresponding to the critical doppler frequency, according to Eqs. (7) and (9), is

$$\dot{r}_{\max} = \frac{c f_p}{4 f_c} , \quad (10)$$

or from Eqs. (8) and (9)

$$\dot{r}_{\max} = \frac{150 f_p}{f_c} , \quad (11)$$

where  $\dot{r}_{\max}$  is in knots for  $f_p$  in cycles per second and  $f_c$  in megacycles per second. It will be shown in Appendix C that the system of Fig. 1 should be theoretically capable of satisfying Eq. (10) provided the filter  $F_2$  is properly designed.

A doppler resolution criterion is established in Appendix B. This criterion specifies that two adjacent frequency spectra having  $\sin x/x$  patterns are just resolvable if the first zero of the one corresponds to the maximum of the other, and vice versa. From Appendix B, Eq. (B5), for an input observed for  $T$  seconds the doppler resolution,  $\Delta F$ , in cycles per second is

$$\Delta F = \frac{1}{T} , \quad (12)$$

and hence the input range-rate resolution,  $\Delta \dot{r}$ , from Eq. (7) is

$$\Delta \dot{r} = \frac{c}{2 f_c T} . \quad (13)$$

From Eq. (8) we have

$$\Delta \dot{r} = \frac{300}{f_c T} , \quad (14)$$

where  $\Delta \dot{r}$  is in knots for  $f_c$  in megacycles per second and  $T$  in seconds. Examining Eqs. (12) and (13) closely we see that the range-rate resolution is a function of the doppler frequency spread,  $\Delta F$ , which in turn exists as a result of the finite observation time,  $T$ . This is really nothing more than an expression of the uncertainty relationship between frequency and time.

Up to this point only the input doppler and range rate have been considered. Now we must look at the effect of the sampling and storage system on the output doppler and range rate. The short-sample technique has already been discussed. The sample pulses are of much shorter duration than the original transmitted pulses and they are repeated at the same rate. Hence, in accord with Shannon's sampling theorem, the doppler should not be altered. In the ideal operation of this system with respect to the sampling process,

it has been assumed that we have ideal rectangular pulses. Of course this is not the case in practice, but for the present we are not considering the secondary effects of rounded pulses.

The input samples are stored on the magnetic drum for a period of  $T$  seconds as stated. All of the recorded pulses are read out from storage in a single drum rotation. The pulses stored in any one range gate are read off in  $\delta$  seconds. Thus the pulses which required  $T$  seconds to record are read out in  $\delta$  seconds, producing a multiplication in doppler frequency of

$$m = \frac{T}{\delta} . \quad (15)$$

If we denote the output quantities by primes, then the output doppler is

$$F' = mF \quad (16)$$

and the theoretical maximum output doppler from Eq. (9) is

$$F'_{\max} = mF_{\max} = \frac{Tf_p}{2\delta} . \quad (17)$$

The output doppler corresponding to a target whose range rate is  $\dot{r}$  knots is

$$F' = \frac{m\dot{r}f_c}{300} , \quad (18)$$

where  $F'$  is in cycles per second for  $f_c$  in megacycles per second. The output doppler resolution from Eqs. (12), (15), and (16) is

$$\Delta F' = m\Delta F = \frac{1}{\delta} . \quad (19)$$

This expression is also verified in Appendix B. From Eq. (18) we have

$$\Delta \dot{r}' = \frac{300\Delta F'}{mf_c} , \quad (20)$$

which yields

$$\Delta \dot{r}' = \frac{300}{f_c T} \quad (21)$$

when combined with Eqs. (15) and (19). Hence, the range-rate resolution remains constant throughout the system as it should:

$$\Delta \dot{r} = \Delta \dot{r}'$$

from Eqs. (14) and (21). Equation (20) provides a measure of the range-rate resolution as a function of the output doppler.

The local oscillator beating with the drum output sweeps one doppler gate for each drum rotation. If the output doppler ranges from 0 to  $F'_{\max}$ , if the output doppler resolution is  $\Delta F'$ , and if the L.O. sweeps  $\Delta F'$  cycles in  $\tau$  seconds, the total number of doppler gates is given by

$$n = \frac{F'_{\max}}{\Delta F'} = \frac{Tf_p}{2} , \quad (22)$$

from Eqs. (17) and (19). A discussion of whether or not this represents the optimum will be found in the section on bandwidth requirements, which is based upon Appendix C.

## STORAGE REQUIREMENTS

Let us consider the cylindrical magnetic drum illustrated in Fig. 7. Assume that the drum is rotating about the axis at a speed synchronized to the transmitter. Let us define

$L$  = circumference of drum

$d$  = diameter of drum

$l$  = length of one storage position

$f_s$  = drum cycling rate

$v$  = velocity of storage circulation

$p$  = total number of storage positions.

Then the following relationships hold:

$$L = \pi d = \frac{v}{f_s} = lp. \quad (23)$$

For the case under consideration of one drum rotation per transmitted pulse,  $f_s = f_p$ , therefore

$$v = f_p lp. \quad (24)$$

The total storage time has been set at  $T$ ; hence the number of pulses integrated, or stored per range gate, is

$$I = f_p T, \quad (25)$$

and the total number of storage positions required for all  $g$  range gates is

$$p = gI = gf_p T. \quad (26)$$

The maximum width of our sampling pulses can now be determined. Assuming that the pulses can be placed side by side, with no spacing between pulses, the sample pulse width,  $\delta_s$ , is given by

$$\delta_s = \frac{\delta}{I}. \quad (27)$$

As described before, the ideal system calls for the oldest single pulse in each range gate to be erased, yielding to the latest or newest pulse. It might be anticipated that such a feat, without destroying adjacent pulses, would be extremely difficult if not impossible to accomplish. A little thought on the matter reveals that, for  $I$  very large, the destruction of a few of the oldest pulses does not significantly disturb the system operation — it merely lessens the effective integration time slightly.

## BANDWIDTH REQUIREMENTS

In this section the bandwidth requirements of the various parts of the system will be determined with reference to the numbered points in Fig. 1. At point 1 the bandwidth will

be dictated by the pulse width. In most search radar systems the pulse shape is not particularly significant. However, in the system presented here it may turn out that for the proper operation of the sampling process the pulse shape may be rather critical. The original ideal concept of this sampling system was based on flat-top rectangular pulses. In practice, of course, this is not a demand consistent with realizing a high signal-to-noise ratio. The pulses will not be flat and this will cause some deterioration in resolution. An analysis of just how much this will deteriorate the resolution of the system has not been made — it is a point that may best be determined experimentally. Perhaps the most that can be said about the bandwidth at point 1 is that it must be at least

$$B_1 \geq \frac{1}{\delta}, \quad (28)$$

and then at point 2 we must have a video bandpass from dc to

$$B_2 = \frac{B_1}{2}. \quad (29)$$

The output bandpass from the sampling mixer is dictated by the sample pulse width,  $\delta_s$ . The fidelity or sharpness which these pulses must possess in order to be recorded accurately on the drum will depend on the drum itself, but in any case the bandpass at point 3 should surely be

$$B_3 \geq \frac{1}{\delta_s} \quad (30)$$

for adjacent spacing. Assuming  $f_s = f_p$ , the output (point 4) requires a bandwidth from dc up to

$$B_4 = F'_{max}, \quad (31)$$

which, to prevent ambiguous range-rate information, must not exceed  $1/2 \delta_s$ . The requirements of the output bandwidth at points 5 and 6 are determined in Appendix C. To permit maximum doppler resolution we must have

$$\frac{1}{4\delta} \leq B_5, \quad B_6 \leq \frac{1}{2\delta}. \quad (32)$$

#### DYNAMIC RANGE REQUIREMENT

One of the most important considerations in this system is the dynamic range required; this can be determined from a study of how the signal-to-noise ratio changes through the system, considering receiver noise only. From the sensitivity viewpoint we can let the input to the receiver consist of an infinite sequence of r-f pulses of duration  $\delta$  and spacing  $\tau$ . After these pulses are contaminated with band-limited additive receiver noise,  $N_i(t)$ , we have at the input to the system

$$E_i(t) = AG(t)\cos(\omega_c + \omega_D)t + N_i(t), \quad (33)$$

where  $G(t)$  is the pulse shaping factor,  $\omega_c = 2\pi f_c$ , and  $\omega_D$  is the doppler angular frequency explained in Appendix A. Both the echo and the noise are multiplied in mixer  $X_1$  of Fig. 1 by the reference signal

$$E_r(t) = \cos\omega_c t, \quad (34)$$

and the resultant is filtered so as to remove terms of the order of twice the carrier frequency. In this process both the signal and noise suffer a 6-db reduction, and hence

the signal-to-noise ratio at point 2 remains the same as at the input. The output at point 2 can be represented from Appendix A as

$$E_2(t) = A_2 G(t) \cos \omega_D t + N(t), \quad (35)$$

where  $N(t)$  is band-limited video noise.

The output at point 3 is the result of sampling the bipolar video, here expressed in Eq. (35), with very short pulses. If we let  $g(t)$  represent the sampling process, the voltage at point 3 can be written as

$$E_3(t) = A_2 g(t) \cos \omega_D t + g(t)N(t), \quad (36)$$

where the  $G(t)$  has disappeared since it is always unity whenever  $g(t)$  exists. The process of record, storage, and read-off alters the frequency response of the stored voltage in such a way as to multiply all modulation frequencies by  $m$ ; hence the voltage appearing at point 4 is

$$E_4(t) = A_2 g(t) \cos m \omega_D t + g(t)N(t). \quad (37)$$

There should be no change in the signal-to-noise ratio as a result of the storage operation, merely a modulation frequency multiplication.

In order to determine any possible change in the signal-to-noise ratio from point 4 on, it is important to study the frequency spectrum of the output from the drum. The spectra for both the signal and the noise are derived in Appendices B and C and are plotted in Fig. 9 for adjacent pulse spacing. The spread about the doppler frequency is due to the fact that we have a finite observation time; this is discussed in Appendix B. If the bandpass of the drum output prior to beating with the L.O. is set at  $F'_{\max} = mf_p/2$  or  $1/2\delta_s$  there should be no appreciable change in the signal-to-noise ratio. Again referring to Fig. 9, it has been established\* that over 90 percent of the signal power is contained between

$$mf_D - \frac{1}{\delta} \leq f \leq mf_D + \frac{1}{\delta}$$

or in a  $2/\delta$  bandwidth. After mixing, the proper output filter bandwidth will be a function of exactly where the L.O. is centered with respect to  $mf_D$  as the drum rotates. Should exact centering exist, the correct output bandpass from the sensitivity viewpoint would be  $1/2\delta$ . This would pass nearly all of the signal but would eliminate noise power in the ratio of  $\delta/\delta_s$ . One cannot expect that the L.O. will be centered exactly, so on the average a 3-db loss in signal power can be expected, as explained in Appendix C. Hence, the expected gain in mean power signal-to-noise ratio should be

$$G \cong \frac{\delta}{2\delta_s} = I. \quad (38)$$

It would appear logical to expect a system power gain in sensitivity proportional to the number of pulses integrated.

The full-wave rectifier after point 5 is the first point in the system where a detector loss could occur. However, at this point in the system all of the integration has been performed and if the signal is not already above threshold at this stage there is no possibility of recovery in any case.

\* S. F. George and A. S. Zamanakos, "Comb Filters for Pulsed Radar Use," Proc. I. R. E. 42:1159 (1954)

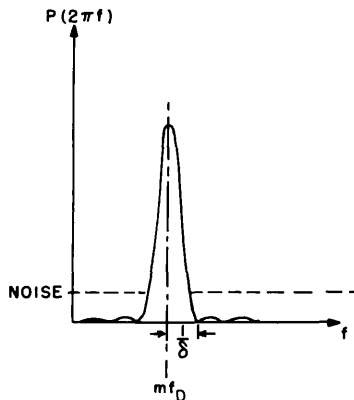


Fig. 9 - Power spectrum at point 4

**A NUMERICAL EXAMPLE**

In order to develop a practical feeling for the equations, let us consider a numerical example of a system operating at a carrier frequency,  $f_c$ , of 40 Mc. Assume transmitted pulses of duration,  $\delta$ , 100  $\mu$ sec and a prf,  $f_p$ , of 200 pps, so that the duty factor is approximately 0.02. Then from Eq. (2) the maximum, unambiguous range is

$$r_{max} = 410 \text{ nautical miles,}$$

using standard single-frequency pulse-radar techniques. From Eq. (3) the number of range gates could be set as

$$g = 50 \text{ gates.}$$

The range resolution is given by Eq. (5) as

$$\Delta r = 8.2 \text{ nautical miles.}$$

Considering a storage drum rotating at the same rate as the pulse repetition rate, the maximum possible unambiguous doppler frequency is given by Eq. (9) as

$$F_{max} = 100 \text{ cps}$$

which corresponds to a target radial velocity, from Eq. (11), of

$$\dot{r}_{max} = 750 \text{ knots.}$$

The doppler resolution is established by the permissible observation or integration time, which in turn is determined by target velocity (i.e., the target must not move out of the range gate) and by the coherence of the echo (i.e., the correlation time). At this writing, there is some indication that the echo may remain correlated for at least 6 seconds and there is speculation that some target returns may have correlation times as high as 20 seconds. From Eq. (12) the doppler resolution for 6-second and 20-second integration times are respectively

$$\Delta F = 1/6 \text{ cps and } 1/20 \text{ cps}$$

corresponding to range-rate resolutions, from Eq. (14), of

$$\Delta \dot{r} = 1.25 \text{ knots and } 0.375 \text{ knot.}$$

In the remainder of this example the 6-second observation time will be used. The frequency multiplication of doppler in the system, given by Eq. (15), is

$$m = 60,000$$

and hence the maximum output doppler will be, from Eq. (17),

$$F'_{\max} = 6 \text{ Mc.}$$

This means that a target whose radial velocity is 750 knots will show up as an output doppler of 6 Mc. From Eq. (19) the output doppler resolution is

$$\Delta F' = 10 \text{ kc}$$

and the output range-rate resolution, from Eq. (21), is

$$\Delta \dot{r}' = 1.25 \text{ knots}$$

which is the same as the input range-rate resolution as previously mentioned. The total number of doppler gates, from Eq. (22), is

$$n = 600 \text{ gates}$$

which is based upon the local oscillator sweeping 10 kc every drum rotation.

The storage requirements are as follows: For a 6-second integration time, the total number of stored samples per range gate is, from Eq. (25),

$$I = 1200.$$

Thus, from Eq. (26), the total number of storage positions required for all 50 range gates is

$$p = 60,000 \text{ positions.}$$

If it can be assumed possible to crowd 2,000 pulses per inch on a drum using contact heads, then

$$l = 1/2000 = 0.0005 \text{ inch}$$

$$L = 30 \text{ inches}$$

$$d = 9.5 \text{ inches}$$

$$v = 6,000 \text{ inches per second.}$$

From Eq. (27) the maximum width of the sampling pulses is

$$\delta_s = 0.083 \mu\text{sec}$$

for side-by-side storing. The bandwidth out to the first zero for such a pulse would be 12 Mc.

The bandwidth requirements, Eqs. (28)-(32), would be

point 1	10 kc
point 2	5 kc
point 3	12 Mc
point 4	6 Mc
point 5	between 2.5 and 5 kc
point 6	between 2.5 and 5 kc.

From Eq. (38) the dynamic range or signal-to-noise ratio improvement is approximately 31 db.

### AZIMUTH DETERMINATION

The measurement of angle of arrival of echo signals requires two or more receiving channels, with overlapping antenna patterns. Each receiving channel requires its own track, with recording and read-out heads on the drum. Angle resolution depends on the number and directivity patterns of the receiver channels. Since target resolution in range rate is very great, angle resolution, at least for moving targets, may be of only secondary importance and may be dictated by other factors, such as antenna size required for given sensitivity specifications or pattern directivity requirements imposed by jamming considerations. Complete 360-degree azimuth coverage could be accomplished by using four simultaneous channels, one for each of the four quadrants. For this case, four separate receiver and correlator systems would be required, the samples being stored on four channels of the same magnetic drum. The display might take the form shown in Fig. 10. Here the rectified outputs from the separate channels would be applied directly to the four plates of the cathode-ray tube, and the sum of the four used for unblocking the tube.

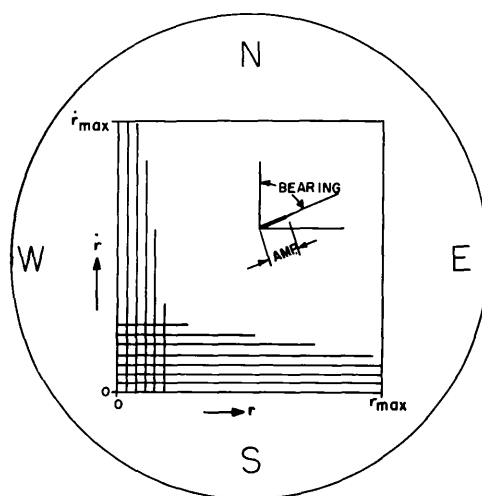


Fig. 10 - Indicator showing possible target bearing

### CONCLUDING REMARKS

The fundamental concepts of a magnetic drum storage system for use in a surveillance radar have been presented along with a numerical example of the parameters which might be employed in one specific application. The success of this system depends upon the degree to which the magnetic drum can be perfected. At the time of this writing the development of drum techniques is under contract to the General Electric Company, contract NONR 1771(00).

## ACKNOWLEDGMENTS

The authors wish to express their appreciation for the valuable assistance of J. P. Barry, A. S. Zamanakos, and C. E. Corum, all of the Mathematics Staff, Radar Division, Naval Research Laboratory, in the preparation of the material and illustrations for this report.

\* \* \*

APPENDIX A  
Obtaining The Doppler Frequency

Assume a train of r-f pulses impinging upon a target which is moving away from the radar with a velocity  $v_T$ . If the pulses are transmitted with a period  $\tau$ , then the time interval between successive received pulses will be  $\tau + \Delta\tau$ , where

$$\Delta\tau = \frac{2v_T\tau}{c} \quad (A1)$$

is the time required for the latter pulse to traverse twice the distance the target has traveled in time  $\tau$ , and  $c$  is the velocity of propagation of the radar wave. Hence, compared with some arbitrary zeroth pulse, the  $i$ th pulse returns at a time

$$t_{iR} = \frac{2r_0}{c} + i\tau + \frac{2v_T i\tau}{c} . \quad (A2)$$

At point  $X_1$  (Fig. 1) this  $i$ th pulse is multiplied by a recirculated transmitted pulse which begins at  $t_{i\tau} = \phi + i\tau$ , where  $\phi$  represents the start of the particular range gate in which the received pulse exists. Neglecting for the present the fact that the pulses exist for only a finite time, the received pulse is of the form

$$E_R = A_R \cos \omega_c \left( t + \frac{2r_0}{c} + i\tau + \frac{2v_T i\tau}{c} \right) \quad (A3)$$

and the reference pulse is of the form

$$E_T = A_T \cos \omega_c (t + \phi + i\tau) . \quad (A4)$$

The resultant output from  $X_1$  is therefore

$$E_0 = A_R A_T \cos \omega_c \left( t + \frac{2r_0}{c} + i\tau + \frac{2v_T i\tau}{c} \right) \cos \omega_c (t + \phi + i\tau) \quad (A5)$$

which can be rewritten as

$$E_0 = \frac{A_R A_T}{2} \left[ \cos \omega_c \left( \frac{2r_0}{c} - \phi + \frac{2v_T i\tau}{c} \right) + \cos \omega_c \left( 2t + \frac{2r_0}{c} + \phi + 2i\tau + \frac{2v_T i\tau}{c} \right) \right] . \quad (A6)$$

Filtering out terms of the order of  $2\omega_c t$  and calling the phase  $\phi' = 2r_0/c - \phi$  we have

$$E_A = \frac{A_R A_T}{2} \cos \omega_c \left( \frac{2v_T i\tau}{c} + \phi' \right) . \quad (A7)$$

Equation (A7) is interpreted to mean that the amplitude of the video pulses coming out at point 2 of Fig. 1 is a function of the doppler frequency

$$\omega_D = \frac{2\omega_c v_T}{c}, \quad (\text{A8})$$

the  $i\tau$  term being taken to indicate samples  $\tau$  seconds apart. It is seen from Eq. (A7) that the amplitude of the video pulses, obtained by letting  $i$  take on successive integral values, varies in accordance with the target velocity and is a function of the constant phase relationship between the received and reference pulses.

If we let  $\omega_D = 2\pi F$  and  $\omega_c = 2\pi f_c$  then

$$F = \frac{2f_c v_T}{c}. \quad (\text{A9})$$

The value of  $c$  in knots is  $5.9 \times 10^8$ . Hence, where  $v_T = \dot{i}$ , and for  $\dot{i}$  in knots and  $f_c$  in megacycles per second,

$$F \cong \frac{\dot{i} f_c}{300} \text{ cycles.} \quad (\text{A10})$$

That a coherent oscillator can be used instead of a recirculated reference pulse to obtain the doppler is easily demonstrated. Instead of Eq. (A4) the reference signal is now

$$E_T = A_T \cos \omega_c (t + \psi). \quad (\text{A11})$$

Hence the output at point 2 is

$$E_a = \frac{A_R A_T}{2} \cos \omega_c \left( \frac{2v_T i \tau}{c} + i\tau + \psi' \right), \quad (\text{A12})$$

where again  $\psi' = 2r_0/c - \psi$ . This is the same as Eq. (A7) provided  $\tau$  is a period of the carrier frequency or provided the pulses are generated in phase coherence, because

$$\cos \omega_c (A + i\tau) \equiv \cos \omega_c A$$

if  $\tau$  is a period of  $\omega_c$  or if  $\omega_c \tau = 2\pi$ . This proves that a coherent oscillator will work instead of recirculated pulses for obtaining doppler.

\* \* \*

**APPENDIX B**  
**Resolution Criterion**

It is a well-known fact that the ability to resolve two adjacent frequencies depends upon the length of time that one is permitted to make observations. In infinite time a sinusoidal wave can be perfectly resolved; whereas in a finite time there appears to be a frequency spread centered about the true frequency. Let us consider the input doppler frequency,  $\omega_D$ , for a time  $T$  as illustrated in Fig. B1. Here

$$\begin{aligned} f(t) &= A \cos \omega_D t, & -\frac{T}{2} < t < \frac{T}{2} \\ &= 0, & \text{elsewhere.} \end{aligned} \tag{B1}$$

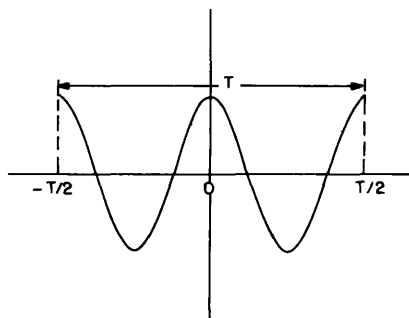


Fig. B1 - Doppler frequency sample

Then the frequency spectrum is given by the Fourier transform

$$F(\omega) = \frac{1}{2\pi} \int_{-\infty}^{\infty} f(t) \cos \omega t \, dt. \tag{B2}$$

Upon introducing Eq. (B1) this becomes

$$\begin{aligned} F(\omega) &= \frac{1}{2\pi} \int_{-T/2}^{T/2} A \cos \omega_D t \cos \omega t \, dt \\ &= \frac{A}{2\pi} \left[ \frac{\sin(\omega - \omega_D) \frac{T}{2}}{\omega - \omega_D} + \frac{\sin(\omega + \omega_D) \frac{T}{2}}{\omega + \omega_D} \right]. \end{aligned} \tag{B3}$$

Thus we see that the spread of frequencies due to a finite observation time has a  $\sin x/x$  form centered about  $\omega_D$ .

Figure B2 shows the resolution criterion that is generally adopted by engineers. The two frequencies  $\omega_1$  and  $\omega_2$  are resolvable, as shown, whenever their separation is at least sufficient that the maximum of the  $\sin x/x$  spread of one comes at the first zero of the other. The resolution from Eq. (B3) is therefore determined by setting  $(\omega - \omega_D)T/2 = \pi$ . This gives

$$\Delta\omega = \omega - \omega_D = \frac{2\pi}{T}, \quad (\text{B4})$$

and hence the frequency resolution is

$$\Delta F = \frac{1}{T} \text{ cycles}, \quad (\text{B5})$$

for a T-second integration time.

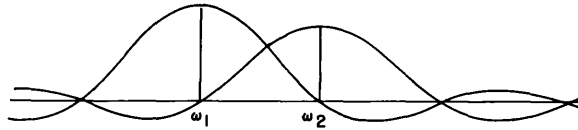


Fig. B2 - Resolution criterion

Let us next consider the resolution of the output doppler at point 4 in Fig. 1. Here we have short-sample pulses of duration  $\delta_s$  and period  $\tau_s$  modulated by a doppler  $m\omega_D$ . There are I pulses in a period  $\delta$  seconds long. To simplify the mathematics let us assume that we have an odd number of pulses and that the doppler frequency is an even function. As before, Eq. (B2) holds, where for positive t

$$\begin{aligned} f(t) &= A \cos m\omega_D t, & k\tau_s - \frac{\delta_s}{2} < t < k\tau_s + \frac{\delta_s}{2} \\ &= 0, & \text{elsewhere,} \end{aligned} \quad (\text{B6})$$

and

$$k = 0, 1, 2, \dots, I/2 \text{ (approximation since } I \text{ is even).}$$

Therefore

$$\begin{aligned} F(\omega) &= \frac{A}{\pi} \left[ \int_0^{\delta_s/2} \cos m\omega_D t \cos \omega t \, dt \right. \\ &\quad + \int_{\tau_s - \delta_s/2}^{\tau_s + \delta_s/2} \cos m\omega_D t \cos \omega t \, dt \\ &\quad + \dots \\ &\quad \left. + \int_{I/2 - \delta_s/2}^{I/2 + \delta_s/2} \cos m\omega_D t \cos \omega t \, dt \right]. \end{aligned} \quad (\text{B7})$$

Considerable manipulation and summation of series finally yields

$$F(\omega) = \frac{A\delta_s}{4\pi} \left[ \frac{\sin(\omega - m\omega_D)\delta_s/2}{(\omega - m\omega_D)\delta_s/2} \cdot \frac{\sin I(\omega - m\omega_D)\tau_s/2}{\sin(\omega - m\omega_D)\tau_s/2} \right. \\ \left. + \frac{\sin(\omega + m\omega_D)\delta_s/2}{(\omega + m\omega_D)\delta_s/2} \cdot \frac{\sin I(\omega + m\omega_D)\tau_s/2}{\sin(\omega + m\omega_D)\tau_s/2} \right]. \quad (\text{B8})$$

Comparison of Eq. (B8) with the work of George and Zamanakos\* shows that the spectrum would be the same as that obtained from a finite sequence of I pulses of equal amplitude except that there are two superimposed  $\sin x/x$  patterns of half amplitude, one shifted up and one down by the doppler frequency  $m\omega_D$ . If the number, I, of pulses in the sequence is large, the patterns will not overlap, as is shown in the reference.

From Eq. (B8) and the reference, the first minimum of the pattern centered at  $\omega = m\omega_D$  occurs when

$$I(\omega - m\omega_D) \frac{\tau_s}{2} = \pi. \quad (\text{B9})$$

The output doppler resolution is therefore

$$\Delta F' = \frac{\omega - m\omega_D}{2\pi} = \frac{1}{I\tau_s}. \quad (\text{B10})$$

For  $\tau_s = \delta_s$  we have

$$\Delta F' = \frac{1}{I\delta_s} = \frac{1}{\delta}, \quad (\text{B11})$$

from Eq. (27). This agrees with Eq. (19) of the text.

---

\* S. F. George and A. S. Zamanakos, "Comb Filters for Pulsed Radar Use," Proc. I.R.E. 42:1159 (1954)

APPENDIX C  
Power Spectra

The frequency spectrum of the sampled doppler coming off the drum at point 4 in Fig. 1 has been determined in Appendix B and is given by Eq. (B8). From this the power spectrum of the signal is easily plotted, as in Fig. 9, for side-by-side pulse positioning on the drum. The power spectrum of white noise after sampling remains flat over the region of concern here. The output of the  $X_3$  multiplier (Fig. 1) is the result of beating the time function whose power spectrum is given in Fig. 9 by a continuously varying L.O. signal which varies by increments of  $1/\delta$  cycles per  $\tau$  seconds. An exact analysis of this process is complex and hence the simplifying assumption is made that the L.O. frequency remains constant during the  $\delta$ -second interval of doppler persistence (one range gate). Two cases are then considered: The first assumes that the L.O. is exactly at the doppler frequency and the second assumes that the L.O. is at the doppler frequency  $\pm 1/2\delta$ . The output power spectrum from  $X_3$  is plotted in Fig. C1 for these two cases. It can be seen that the filter  $F_2$  with cutoff at  $1/2\delta$  would pass nearly all of the signal power in case 1, whereas in case 2 it would remove over half the power. Hence there is an average loss in sensitivity of about 3 db in this filter. However, the resolution called for in Eq. (19) cannot be attained with  $F_2$  cutoff at  $1/2\delta$  since both sidebands are being passed. In order to achieve the maximum resolution of Eq. (19) it is required that the cutoff of  $F_2$  be reduced to somewhere between  $1/2\delta$  and  $1/4\delta$ .

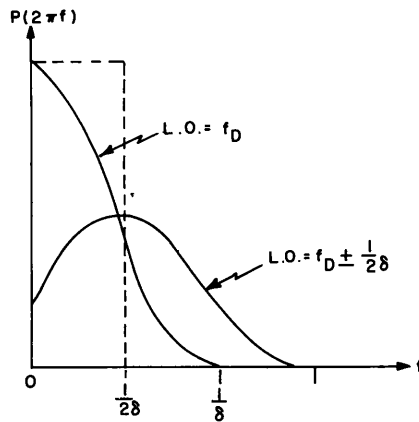


Fig. C1 - Output power spectra  
before  $F_2$

\* \* \*

## LIST OF SYMBOLS

$B_k$	bandwidth at point k in Fig. 1
$d$	diameter of storage drum
$f_c$	transmitted carrier frequency
$f_D$	doppler frequency = F
$f_p$	pulse repetition frequency
$f_s$	storage cycling rate
$F$	input doppler frequency
$F_2$	bandwidth of output filter
$\Delta F$	input doppler resolution
$F'$	output doppler frequency
$\Delta F'$	output doppler resolution
$g$	number of range gates
$g(t)$	sampling pulse factor
$G$	system gain in signal-to-noise ratio
$G(t)$	shaping factor on input pulses
$I$	total number of pulses integrated
$l$	length of one storage position
$L$	circumference of storage drum
$m$	frequency multiplication factor
$n$	number of resolvable doppler gates
$N_i(t)$	band-limited input noise
$N(t)$	band-limited video noise
$P$	total number of storage positions
$r_{max}$	maximum range obtainable

$\Delta r$	range resolution
$\dot{r}$	radial velocity of target = $v_T$
$\Delta \dot{r}$	range-rate resolution
$T$	total storage or integration time
$v$	velocity of storage circulation
$v_T$	radial velocity of target
$\delta$	transmitted pulse duration
$\delta_s$	duration of sample pulses
$\tau$	transmitted pulse repetition period
$\omega_c$	transmitted angular carrier frequency = $2\pi f_c$
$\omega_D$	angular doppler frequency = $2\pi f_D = 2\pi F$

\* \* \*